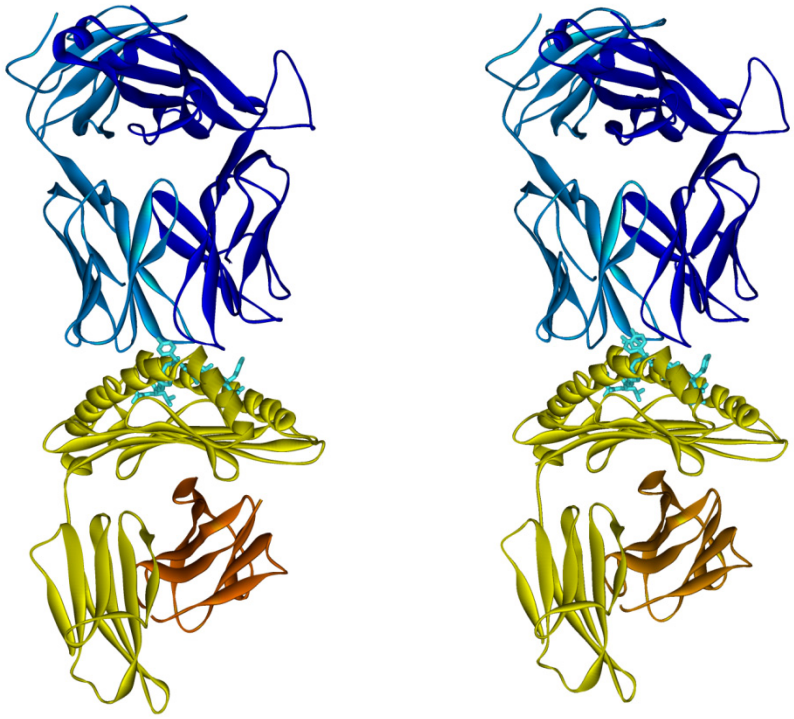

Figure S1. Structural overviews of the A6-Tax-Y5F$_{4F}$/HLA-A2 structure (left) A6-Tax-Y5F$_{34FF}$/HLA-A2 structure (right).

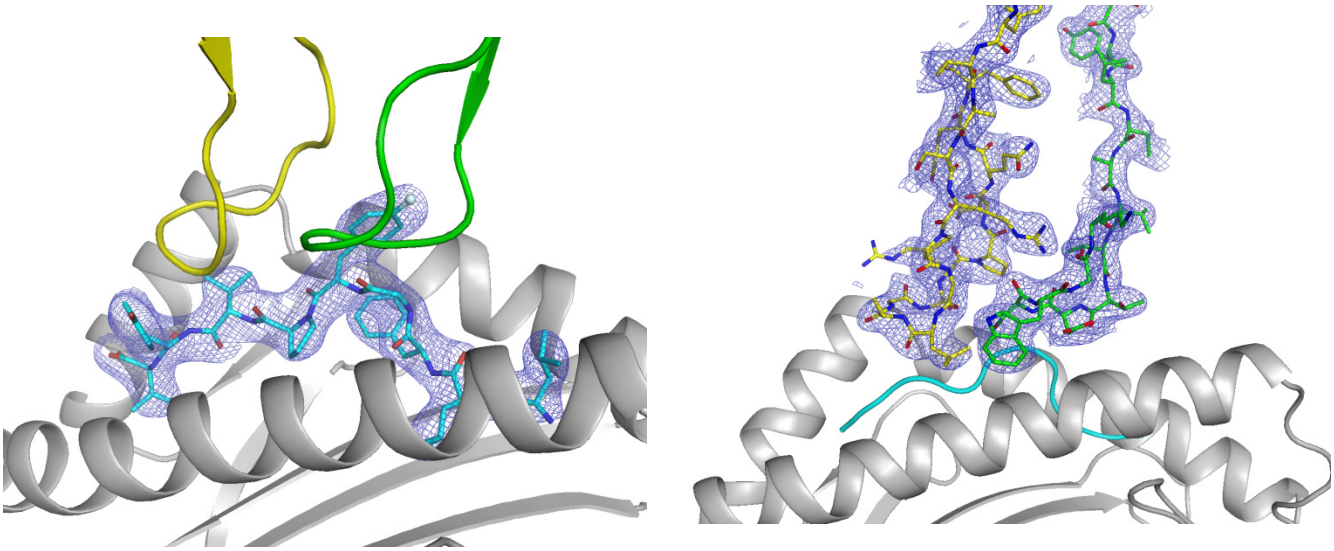

Figure S2. 2Fo-Fc electron density for the peptide (left) and the CDR3 loops (right) in the A6-Tax-Y5F$_{4F}$/HLA-A2 structure.

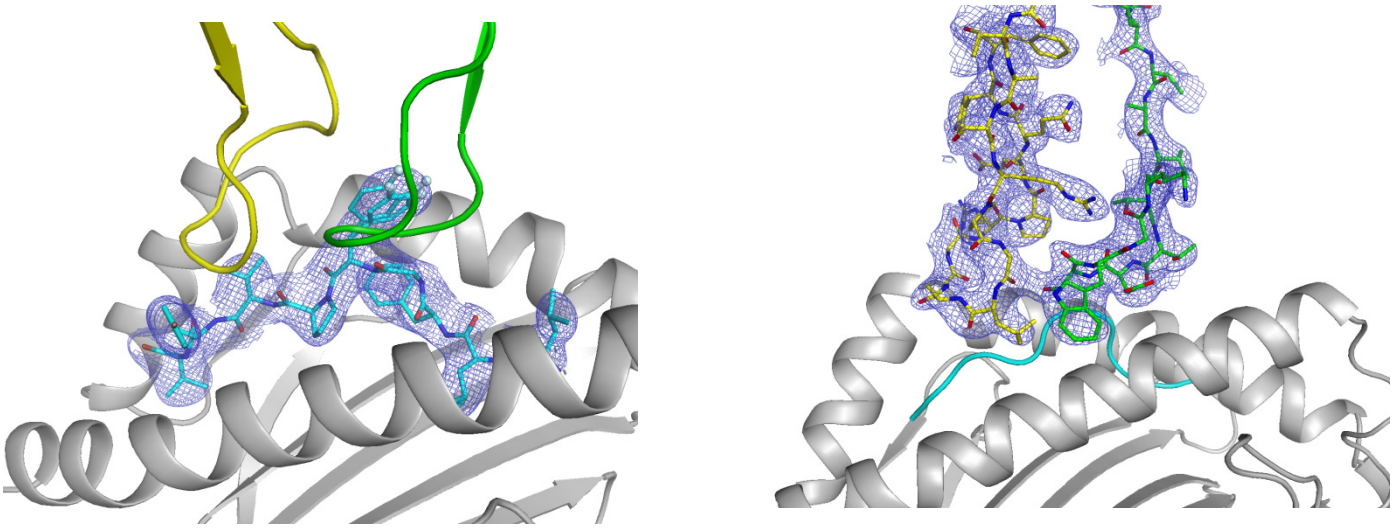

Figure S3. 2Fo-Fc electron density for the peptide (left) and the CDR3 loops (right) in the A6-Tax-Y5F$_{34FF}$/HLA-A2 structure.

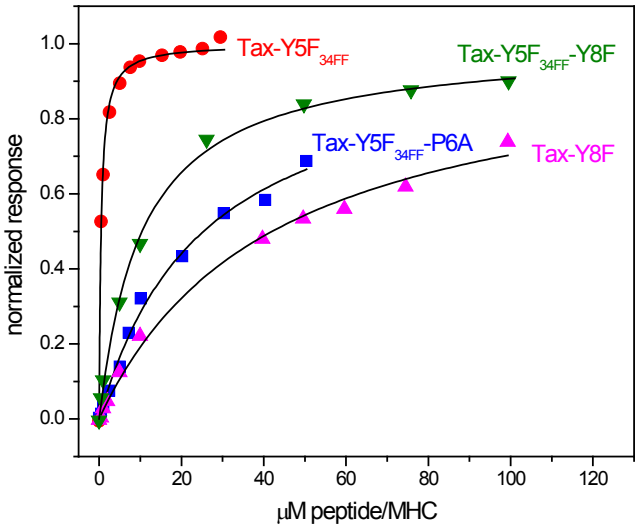

Figure S4. Biacore equilibrium binding data for A6 recognition of the doubly-substituted Tax-Y5F$_{34FF}$-Y8F (green) and the Tax-Y5F$_{34FF}$-P6A (blue) ligands. For comparison, data for recognition of the singly substituted Tax-Y5F$_{34FF}$ and Tax-Y8F ligands are also shown. Note that although saturation was not reached in all cases, the RUmax for all experiments was predetermined by injecting saturating concentrations of the high affinity Tax-Y5F$_{34FF}$ ligand, increasing the accuracy of the low affinity measurements (see Experimental section).

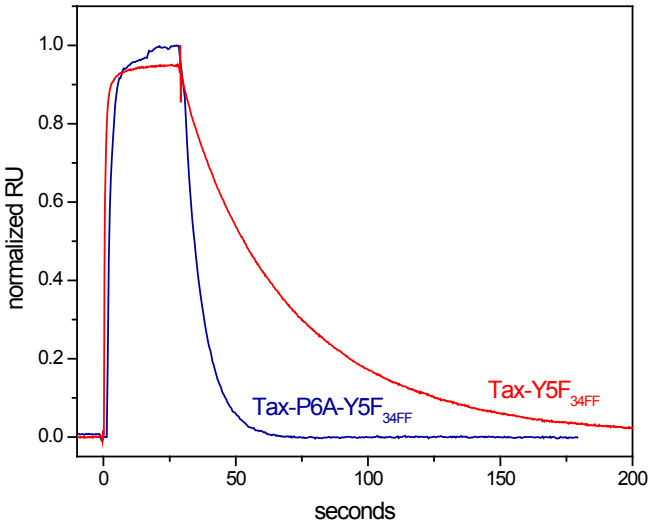

Figure S5. Biacore kinetic data for dissociation of A6 recognition from the doubly-substituted Tax-Y5F$_{FF}$-P6A ligand (blue). For comparison, dissociation from the high affinity Tax-Y5F$_{34FF}$ ligand is shown in red.